Journal of Applied Polymer Science

Spontaneous formation of gold microplates during reduction-coupled removal of noble metals using Dowex M4195 resin

Dorota Jermakowicz-Bartkowiak,[1] Piotr Cyganowski,[1] Anna Leśniewicz,[2] Wlodzimierz Tylus,[3] Jacek Chęcmanowski,[3] Anna Marcinowska[1]

[1]Division of Polymer and Carbonaceous Materials, Faculty of Chemistry, Wroclaw University of Technology, 50-370 Wroclaw, Poland

[2]Division of Analytical Chemistry, Faculty of Chemistry, Wroclaw University of Technology, 50-370 Wroclaw, Poland

[3]Department of Surface Engineering, Catalysis and Corrosion, Faculty of Chemistry, Wroclaw University of Technology, Wybrzeże Wyspianskiego 27, 50-370 Wroclaw, Poland

Correspondence to: P. Cyganowski (E-mail: piotr.cyganowski@pwr.edu.pl)

ABSTRACT: The present work reports the novel phenomenon of spontaneous formation of gold microplates. The effect is observed as a consequence of $AuCl_4^-$, $PtCl_6^{2-}$, $PdCl_4^{2-}$, and ReO_4^- sorption on the Dowex M4195 resin. Therefore an attempt to explain the phenomenon mechanism is made. The research is covering sorption, kinetic and thermodynamic studies. The shapes of formed gold single plates are determined. The uptakes of Au(III), Pt(IV), Pd(II), and Re(VII) tests have been conducted using a batch method from single-component metals solutions in 0.1*M* HCl. The sorption-reduction phenomenon has been assessed by executed SEM, FTIR, XRD, and XPS studies. The greatest sorption capacity, combined with reduction-coupled removal phenomenon, has been achieved for gold (5.5 mmol Au·g^{-1} at 9°C). Executed SEM and XRD analyzes prove formation of gold single crystals during present process, furthermore reduction of rhenium is indicated by XPS analysis. Based on the obtained FTIR and Raman's spectra, the reduction phenomenon is probably followed by resins' functional groups oxidation. © 2015 Wiley Periodicals, Inc. J. Appl. Polym. Sci. **2015**, *132*, 42425.

KEYWORDS: adsorption; nanoparticles; nanowires and nanocrystals; separation techniques

Received 13 January 2015; accepted 28 April 2015

DOI: 10.1002/app.42425

INTRODUCTION

Evolving human society and developing new technologies cause growing amount of waste electrical and electronic equipment (WEEE).[1] The UN Environmental Program estimates that all over the world 20–50 million tons of WEEE a year is generated, and its amount rise three times faster than any other type of wastes.[2] In that circumstances management of e-wastes recently became a serious problem that has been regulated by New European Union Directive 2012/19/EU.[3] Because WEEE is a source of precious metals, recycling of that type of wastes has to be proceeded with use of the most efficient methods,[3,4] that could allow to recover any precious resources. However, present recovery techniques suffer lack of effectiveness.[1,4]

In recent few decades, applications of ion exchangers and chelating resins are the relevant concern of chemical industry.[5] Because of multiple applications, functionalized resins are widely used in waste water treatment,[6] drugs purification,[7] metals separation and recovery,[8,9] and ion chromatography.[10]

Recovery of precious metals on chelating resins is preferred over ion exchange methods because of its efficiency.[11] Chelating resins reveal higher sorption capacity, rate of the sorption process, selectivity of interfering ions, and sensitivity.[5] The phenomenon is attributed to the donor atoms, present in the functional groups of resins, which are able to coordinate metals ions.[12]

It has been recognized that coordinating abilities of the resins allow proceeding sorption processes with great efficiencies even if metals in solutions are present in trace and ultra-trace amounts.[12–14] On the other hand, it has been proven that variety of functionalities, involved into different supports,[15–17] have abilities to reduce gold in its solutions. Furthermore, Changmei[18] has reported spontaneous reduction of Au(III) to Au(0) nanoparticles on novel polystyrene-supported 3-amino-1,2-propanediol chelating resin.

Additional Supporting Information may be found in the online version of this article.

It has been recognized that, during reduction of Au(III) process,[19] next to the gold nanoparticles, obtainment of gold microstructures, especially microplates, is possible. Triangular and hexagonal gold microplates have been widely investigated due to their potential applications in medicine diagnostics, electronics, optics, etc.[20] In recent years, gold single plates were obtained by reduction of Au(III) to Au(0).[21–23] The referred processes were intentional, and most frequently the $NaBH_4$ as the reducing agent was used.

The worldwide literature does not provide information about spontaneous reduction of Au(III) to Au(0) during typical sorption process that results with obtainment of regular microplates. The present paper presents the novel effect of unexpected, unenforced and uncontrolled formation of gold microplates with use of chelating Dowex M4195 resin. Furthermore reduction of ReO_4^-, Re(VII), ion sings were observed. The sorption of Au(III), Pt(IV), Pd(II) chlorocomplexes, and Re(VII) ion was evaluated. Shapes of the obtained gold microplates were determined. The sorption studies were conducted from single-component solutions in 0.1*M* HCl which contained Au(III), Pt(IV), Pd(II) present as chlorocomplexes, and Re(VII) occurred as perrhenate ion (ReO_4^-).

EXPERIMENTAL

In order to pretreat the Dowex M4195 resin for further procedures, ion exchanger was placed in a glass ion exchange column. 1*M* HCl, distilled water, 1*M* NaOH and distilled water was passed through the column, respectively, until the outflow reached neutral pH. Next, the polymer was washed with 0.1*M* HCl and 0.001*M* HCl, respectively.[24]

Reagents and Solutions

The evaluated Dowex M4195 resin was purchased from Aldrich Chemical. All of the reagents used for characterization of the Dowex M4195 resin were purchased from Avantor Performance Materials Poland and used as received. Stock solutions for sorption studies were prepared by dissolving $HAuCl_4{\cdot}3H_2O$ (bought from Avantor Performance Materials Poland), H_2PtCl_6, H_2PdCl_4 (purchased from INNOVATOR), and NH_4ReO_4 in 0.1*M* HCl was acquired in Aldrich Chemical, respectively.

Methods and Materials

Characterization of the Dowex M4195. The centrifugation technique has been applied to measure the 0.001*M* HCl regain, that value is 0.87 $g{\cdot}g^{-1}$.[25]

The nitrogen content was determined as 8.15 $mmol{\cdot}g^{-1}$ using the Kiejdahl's method,[26] applied during studies referred in.[27] Then, ligand content (Z_L), based on amount of nitrogen atoms was calculated.

The content of Cl (2.43 $mmol{\cdot}g^{-1}$) was determined using the Schöniger's method, that has been applied to polymers.[28]

Hecker's procedure was applied for determination of the anion exchange capacity, Z_H (2.18 $mmol{\cdot}g^{-1}$).[29]

The obtained characteristic has been applied as reference values during further studies on sorption of the noble metals and rhenium.

Table I. Applied Single-Component Solutions in 0.1*M* HCl

Initial concentration of metals ($mmol{\cdot}dm^{-3}$)				
Solution	Au	Pt	Pd	Re
1	0.24	0.24	0.25	0.27
2	0.48	0.49	0.49	0.54
3	0.97	1.22	1.24	1.34
4	2.43	2.43	2.46	2.69
5	4.86	4.87	4.92	5.38

Specific solutions were named with use of number of the mixture (1–5) and symbol of a metal that it contains (for example 1-Au).

Sorption of Au(III), Pt(IV), Pd(II), and Re(VII) Studies. Initial concentrations of used single-component solutions were adjusted in order to obtain approximately 0.24–4.9 mmoles of each metal per dm^3. Specific solutions were named with use of a solution number (1–5) and symbol of a metal that it contains (for example 1-Au describes solution 1 with Au(III) complex). Concentrations of used solutions are presented in Table I.

Sorption ability of Au(III) (present as $AuCl_4^-$), Pt(IV) (present as $PtCl_6^{2-}$), Pd(II) (present as $PdCl_4^{2-}$), and Re(VII) (present as ReO_4^- ion) was evaluated with batch method by contacting the Dowex M4195 resin with specific metal solution in 0.1*M* HCl in accordance to procedure previously presented in.[27] Resin was being shaken with specific solution for 48 h at 9, 30, and 50°C, respectively. Next, the polymers were separated by filtration. The concentration of the metals was determined with use of Perkin–Elmer AAnalyst 200 atomic spectrophotometer.[30] Concentration of Re was specified with use of UV/VIS spectroscopy method.[27]

Sorption value was calculated from the mass balance and the initial concentration in the acidic solution. The distribution coefficients (K) were calculated as the ratio of the amount of metal adsorbed by 1 g of resin and the amount of metal remaining in 1 dm^3 of solution after sorption.

The obtained data of Au(III), Pt(IV), Pd(II), and Re(VII) sorption on the Dowex M4195 resin were applied to Langmuir's and Freundlich's mathematical models, respectively:[31]

$$\frac{C_e}{q_e} = \frac{C_e}{Q_0} + \frac{1}{K_L \cdot Q_0}$$

$$\log q_e = \log K_f + \frac{1}{n}\log C_e$$

where C_e is equilibrium of metal ($mg{\cdot}dm^{-3}$), q_e is adsorption capacity in equilibrium state ($mg{\cdot}g^{-1}$), derived from sorption isotherms (Figures 1–3).

Parameters Q_0 (saturated sorption capacity on the resin, $mg{\cdot}g^{-1}$), and K_L (the binding constant, $dm^3{\cdot}mg^{-1}$) were calculated by plotting C_e/q_e versus C_e (Langmuir's mathematical model).

Parameters K_f (Freundlich's parameter, $mg{\cdot}g^{-1}$) and n (dimensionless Freundlich's parameter) were calculated by plotting $\log q_e$ versus $\log C_e$ (Freundlich's mathematical model).

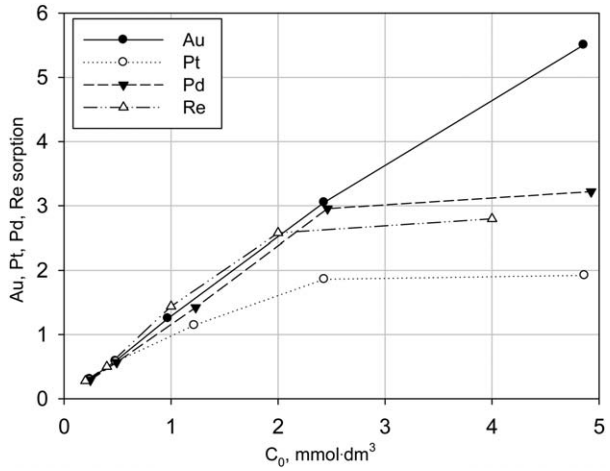

Figure 1. Sorption (mmol·g^{-1}) isotherm from single-component solutions in 0.1*M* HCl at 9°C.

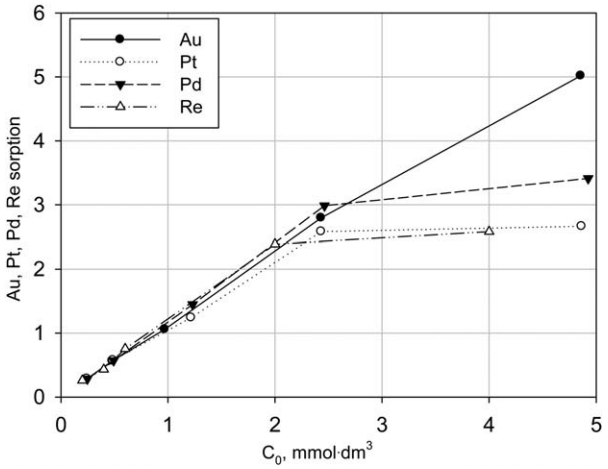

Figure 3. Sorption (mmol·g^{-1}) isotherm from single-component solutions in 0.1*M* HCl at 55°C.

To calculate thermodynamic parameters, the sorption isothermal curves were obtained at 9, 30, and 50°C. In order to calculate free energy (ΔG), enthalpy (ΔH), and entropy (ΔS) of the sorption, partition coefficient K_L (dm^3·mg^{-1}) was varied with change of temperature. K_L parameter was calculated by plotting C_e/q_e versus C_e (Langmuir mathematical model).[32] Free energy of sorption was calculated with use of equation:

$$\Delta G = -RT\ln K_L$$

where R is the gas constant (8.314 J·mol^{-1}·K^{-1}) and T is temperature (K). Equation is equal to.[32]

$$\ln K_L = -\frac{\Delta H}{RT} + \frac{\Delta S}{R}$$

Values of ΔH (kJ·mol^{-1}) and ΔS (J mol^{-1}·K^{-1}) were calculated from the slope and intercept of $\ln K_L$ versus $1{\cdot}T^{-1}$ plot.[32,33]

Due to the fact that kinetics of the sorption process is very important factor from industrial point of view, kinetic studies were proceeded. For this purpose, the Dowex M4195 resin, in a swollen form, in amount equivalent to 0.018 mmol of ligand quantity was introduced into 20 cm^3 glass bottles. Next, 10 cm^3 of the solutions with initial concentrations of 1.46 mmol Au·dm^{-3}, 1.40 mmol Pt·dm^{-3}, 2.46 mmol Pd·dm^{-3}, and 0.54 mmol Re·dm^{-3} were added, respectively. Initial concentrations of the applied solutions were calibrated in way that allowed ensuring full occupation of the functionalities. The resin was being contacted with proper solution for 1–48 h, respectively. After specific time resin was separated by filtration, next concentrations of each metal was determined, and sorption (mg·g^{-1}) was calculated.

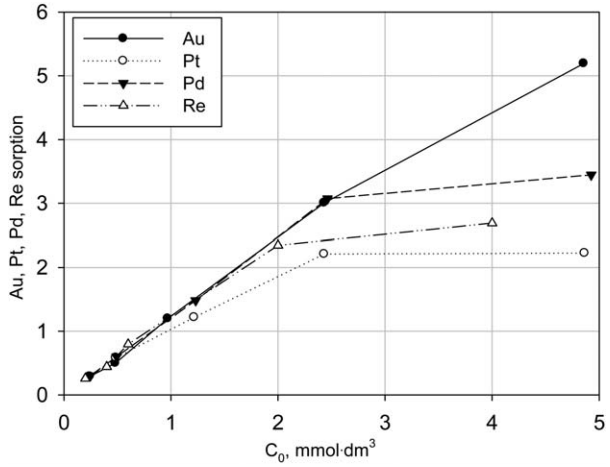

Figure 2. Sorption (mmol·g^{-1}) isotherm from single-component solutions in 0.1*M* HCl at 30°C.

The experimental data of Au(III), Pt(IV), Pd(II), and Re(VII) uptake were applied to Lagergren's, quasi-first-order, and Ho's, quasi-second-order mathematical models, respectively. The interpretation of kinetic behavior was proceeded by calculating kinetic parameters with use of Lagergren's equation,[34,35] in its reduced form, and Ho's equation, respectively:[36]

$$\log(q_e - q_t) = \log q_e - \frac{k_1}{t}\cdot t$$

$$\frac{t}{q_e} = \frac{1}{k_2 q_e^2} + \frac{1}{q_e}\cdot t$$

where t (min) is time, q_e (mg·g^{-1}) is sorption at equilibrium, q_t (mg·g^{-1}) is sorption in time t. Parameter k_1 (min^{-1}) was calculated from slope of $\log(q_e - q_t)$ versus t plot. Parameter k_2 (g·mmol^{-1}·min^{-1}) was obtained from intercept of t/q_e against t plot.[37]

Mechanism of the Sorption. The present process mechanism evaluation was proceeded by determining energy activation that was calculated with use of Arrhenius' eq. (1) in its linear form.[32]

$$\ln k = \ln A + \frac{-E_a}{RT} \quad (1)$$

where k is constant rate from kinetic model which was applied in kinetic studies, A (g·mg^{-1}·min^{-1}) is temperature factor, R (J·mol^{-1}·K^{-1}) is the gas constant, T (K) is temperature. Energy of activation, E_a (kJ·mol^{-1}), was calculated from slope of $\ln k$ versus $1{\cdot}T^{-1}$ plot.

SEM, XRD, FTIR, Raman, and XPS Analyses. The morphology of the Dowex M4195 resin, loaded with Au(III) and Re(VII) was examined by scanning electron microscope JSM 5800LV (SEM). The microscope was equipped with the JSIS 300 Oxford X-ray (EDS) analyzer that made possible determination of the average composition of the surface layer of the sample.

An X-ray powder diffraction method (XRD) was applied for qualitative analysis of structures obtained during noble metals sorption on the Dowex M4195 resin. For that purpose measurements in the symmetric $\theta/2\theta$ Bragg-Brentano geometry using a Philips X'PERT system were done. The analysis procedure has been previously presented in reference.[38]

In order to reveal changes in a chemical structure of the Dowex M4195 resin, the Fourier's Transformation Infrared Spectroscopy (FTIR) and Raman Spectroscopy were performed. The FTIR spectra in KBr pallets were recorded using Perkin-Elmer System 2000 spectrophotometer. Raman transitions were recorded using Bruker RFS100 spectrometer equipped with Nd laser excitation.

X-ray photoelectron spectroscopy was executed on SPECS XPS/AES/UHV System equipped with PHOIBOS 100 spectrometer and SPECLAB software. X-ray source was generated using Mg anode operating at 100 W (wide-range scan) and 150–250 W (high-resolution spectra). (Although to avoid/minimize photoreduction effect during XPS experiments Au(III) spectra were recorded in short time with relatively low power of anode 150 W). The spectrometer energy scale was calibrated using Au($4f_{7/2}$), and Re($4f_{7/2}$) lines. Sample charging was compensated using an electron flood gun with 0.5 mA current and 0.1 eV energy. All spectra were referenced to 284.8 eV (contamination carbon). The base pressure in the UHV analysis chamber was below $5{\cdot}10^{-10}$ mbar. The spectra were collected and curve-fitted by using the SpecsLab software. A nonlinear least-squares fitting algorithm was applied using peaks with a mix of Gaussian and Lorentzian shape and a Shirley baseline.

RESULTS AND DISCUSSION

Sorption Studies

Results obtained during sorption tests from single-component solutions allowed plotting sorption isotherms. All the curves of Au(III), Pt(IV), Pd(II), and Re(VII) uptake are presented in the Figure 1 (sorption at 9°C), Figure 2 (sorption at 30°C), and Figure 3 (sorption at 50°C), respectively.

Basing on calculated values of sorption, S ($mmol{\cdot}g^{-1}$), we have determined that affinity of the uptake of all metals, from single-component solutions was as follows: Au(III)>Pd(II)>Re(VII)>Pt(IV), respectively. Gold sorption achieved the greatest values (5.0–5.5 mmoles of $Au{\cdot}g^{-1}$, Figures 1–3), and no sorption isotherm plateau was observed, which could be caused by observed gold microplates formation phenomenon, discussed below.

Sorption capacity, Z_H (2.18 $mmol{\cdot}g^{-1}$) corresponds to the ligand content Z_L (2.72 $mmol{\cdot}g^{-1}$). In accordance to,[39] the grade which the Dowex M4195 resins functional groups are protonated to, in conditions applied, is two nitrogen atoms. That corresponds to sorption capacities achieved in present studies (Figures 1–3). Palladium (II) chlorocomplex was uptaken with efficiency up to 3.4 mmoles $Pd{\cdot}g^{-1}$ (Figure 3), while Pt(IV) and Re(VII) were removed with much lower amounts, 2.7 mmoles $Pt{\cdot}g^{-1}$ and 2.7 mmoles $Re{\cdot}g^{-1}$, respectively. According to,[40] in most of the processes where solvent extraction is used, flat and square complexes $AuCl_4^-$, $PdCl_4^{2-}$ ions are removed faster, than octahedral platinum complex $PtCl_6^{2-}$ and tetrahedral rhenium ion ReO_4^-. At 30°C sorption of Pd(II) reached 3.4 mmoles $Pd{\cdot}g^{-1}$ (Figure 2), that result was similar to that received by Wolowicz and Hubicki in,[41] where the same resin and experiment conditions were applied.

The investigation revealed sorption of Re(VII) ion (ReO_4^-) ca. 2.7 mmoles $Re{\cdot}g^{-1}$ (Figure 2) which was greater than on commercially available for industrial solutions strongly basic Amberset A920U resin (0.15 mmoles $Re{\cdot}g^{-1}$),[42] and lower than on expanded-gel structure materials based on quaternized poly(4-vinylpiridyne) (1VPJ4) from hydrochloric systems (4.4 mmoles $Re{\cdot}g^{-1}$).[27] In order to verify character of the sorption on the investigated Dowex M4195 resin, Langmuir's and Freundlich's mathematical models were applied to the obtained sorption isotherms.

Formation of Gold Microplates

Present research revealed absence of Au(III) sorption isotherms plateau (Figures 1–3). Instead, after separating the beads of the resin from solutions 4-Au and 5-Au (Table I), reduced gold in its metallic form was present in solutions after sorption process and on the surface of Dowex M4195 resin. According to Mohammadnejad,[43] reduction of Au(III) from hydrochloric solution could be attributed to the existence of defect sites on the silicate surfaces like surface of glass bottles used. However this effect was not reported by Tuzen,[14] who used the same resin and much more less concentrated solution of gold (0.2 mg $Au{\cdot}dm^{-3}$). That suggests that great concentration of gold in used mixtures, could propagate reduction of gold, present as $AuCl_4^-$ to its metallic, microparticle form. It has been recognized, that some of the aromatic amines themselves[44] or those involved into structure of block copolymers,[17,45] suspension amine-functionalized copolymers,[23] and magnetic nanoparticles,[46] as well can have gold-reducing abilities in chloroaureate solutions. All of the mentioned methods require additional reducers, most commonly $NaBH_4$ is used.

Nevertheless, there is possibility that the functional bis(2-pyridylmethyl)amine groups of the Dowex M4195 resin could reduce Au(III) to metallic gold microplates without any additional action. That effect has not been previously reported in the worldwide literature.

In order to identify shape of obtained gold structures, portion of the solution 5-Au (Figure 5), that remained after sorption process, was transferred onto slip cover and analyzed with use of Zeiss Axio Optical Microscopy.

Figure 4 shows structures of observed gold particles that are clearly regular (triangular and hexagonal). In reference to Bolisetty,[47] the fact could suggest that "self-assembling" interactions occurred between functional groups of the Dowex M-4195 resin

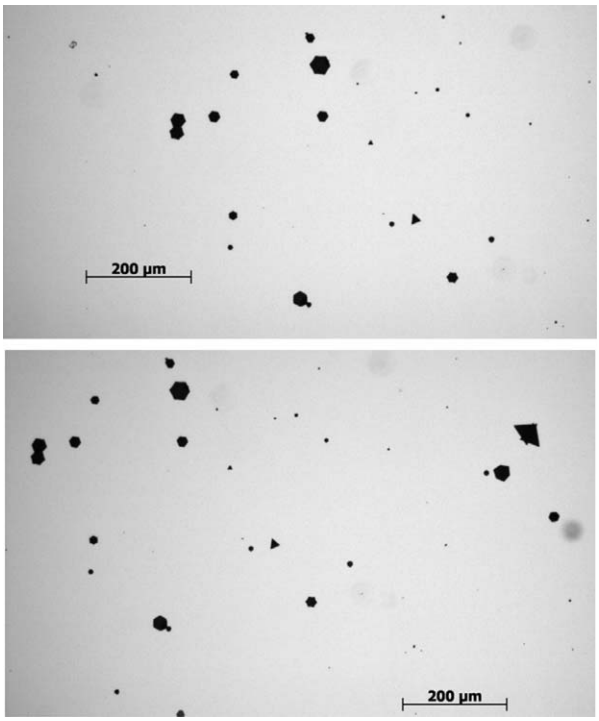

Figure 4. Reduced gold microplates in remaining solution 5-Au.

and Au(III) complex.[47] According to,[48] the size of the formed gold grain is dependent on the initial concentration of the metal in the solution used at the beginning of the process. That could be a reason why reduced gold was not observed after sorption process from solutions 3-Au, 2-Au, and 1-Au (Table I). Phenomenon of gold reduction makes evaluation of Au(III) sorption by the Dowex M4195 resin difficult. There is possibility, that gold was not sorbed on the beads of the resin with the largest amounts in comparison to other metals because high sorption value was probably induced by reduction phenomenon. Absence of gold sorption isotherm plateau suggests that reduction process was still in progress just before resin was separated (Figures 1–3).

In order to confirm that conclusion the gold plates were separated by filtration from solution 5-Au that remained after sorption. Remaining, "clear", solution was placed in a sealed glass probe. After few days gold microplates were observed. Figure 5 displays reduced gold in filtrated and stored 5-Au solution. The effect confirms that reduction of gold Au(III) was still going on in the solution after sorption process even separated from the Dowex M4195 resin. There is possibility that only short contact of gold chlorocomplex $AuCl_4^-$ with functionalities of the Dowex M4195 resin combined with reduction potential of Au(III) (1.002 eV) was enough to begin the process.[49]

The parameters received by analysis of the sorption isotherms, because of the issues discussed below, have been placed in the Supporting Information for Review. Obtained data led draw our attention to the phenomenon that is the subject of this paper. Furthermore, as far as reduction of gold was clearly visible, the anomaly of rhenium sorption would not be noticed if no sorption parameters analysis was proceeded. Therefore, even because of the reduction effect, the sorption models became not relevant, it is necessary to briefly discuss them in order to reveal the cause of the further actions.

As may be seen in the Supporting Information Table S1, the correlation coefficients, R^2, given by applying Langmuir's model, were found in values range 9.143-1.0000, and the dimensionless Langmuir's parameter, R_L, was found in range of 0.01-0.64 indicating appliance of the processes with the Langmuir's model.[31]

The thermodynamic parameters were received by fitting lnK_L (derived from Langmuir's model) versus reciprocal temperature $1{\cdot}T^{-1}$. The positive values of ΔS provided in the Supporting Information Table S2, observed during Pt(IV) and Pd(II) uptake, suggest increasing randomness at the solid-liquid phase. Negative value of entropy in case of Au(III) and Re(VII) sorption indicates, that some chemical reaction (which decreases randomness) could occur during the sorption process (Supporting Information Table S2).[50] In case of Au(III) uptake, mentioned reduction of Au(III) could explain the effect.[32] The entropy is followed by sorption free energy values, ΔG, that are becoming *more negative* with increasing temperature during Pt(IV) and Pd(II) uptake, indicating the rising spontaneity of the process. The opposite effect is observed for Au(III) and Re(VII) loading (Supporting Information Table S2).

As displayed in the Supporting Information Figures S2, S3, and S4, sorption of Re(VII) and Pd(II) reached equilibrium within 8 h at 9, 30, and 55°C. Loading of Au(III) and Pt(IV) was slower and equilibrium was achieved in 12 h. Uptake of Au(III) and Re(VII) decreased with increase of temperature. The obtained data were fitted to quasi-first-order and quasi-second-order kinetic models, the received parameters are placed in the Supporting Information Table S3. The correlation coefficients, R^2, obtained by applying experimental data to Ho's model are close to 1 and are higher than those received from Lagergren's model application. That means that quasi-second-order kinetic model is better fit for present studies. Quasi-second-order rate constant values, k_2, are the highest in case of Re(VII) ion sorption at 9 and 30°C, which suggests that rhenium is sorbed more rapidly than other metals at the investigated temperatures.

Figure 5. Reduced gold in filtrated and stored 5-Au solution.

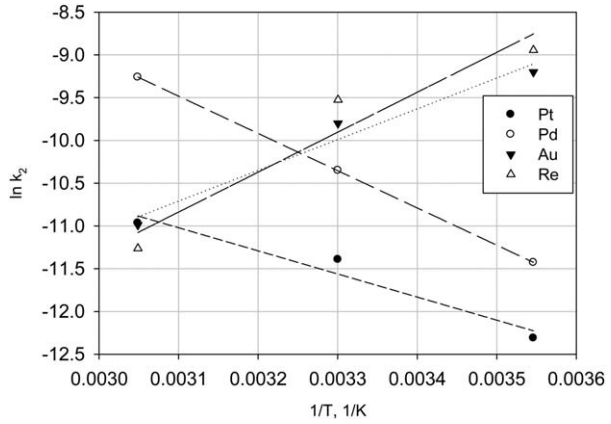

Figure 6. Plot of $\ln k_2$ versus reciprocal temperature for sorption from single-component solutions in 0.1*M* HCl.

The uptake of Re(VII) is an endothermic process, which means that velocity of rhenium sorption should increase with increasing temperature. Instead, the process decreases its rate. In order to explain that phenomenon, an attempt to determine the mechanism of the process has been made.

As a factor, that allowed to determine mechanism of the process, energy activation, E_a (kJ·mol^{-1}), was applied. In order to calculate the energy activation the quasi-second-order kinetic model was used.

Figure 6 shows plot of $\ln k_2$ versus reciprocal temperature $1{\cdot}T^{-1}$. Table II displays calculated values of energy activation for each studied metal.

Negative value of E_a of Au(III) and Re(VII) sorption proves that the higher temperature is the slower the process becomes (Table II).[51] The value of activation energy (E_a) of the gold and rhenium sorption is negative (Au, Re, Table II). In general, the phenomenon indicates, that increase of the temperature of the sorption processes, increases the solubility of gold chlorocomplexes and rhenium ions. As the result, the forces between adsorbates and solvent are stronger, than those between adsorbate (Au, Re) and adsorbent (Dowex M4195).[52]

As far as mentioned reduction of Au(III) to Au(0) to its crystalline form could explain why the gold sorption is exothermic, no similar effect was observed during Re(VII) uptake. Nevertheless value of E_a (−38.83 kJ·mol^{-1}, Table II) of ReO_4^- ion uptake was determined as negative. The negative values of activation energy indicate only the multi-stage nature of the process, and do not give any information about real elementary stages constituting the mechanism of interactions. Hence, the calculated kinetic parameters and activation energies does not provide an appropriate information about the real mechanisms of the Au(III) and Re(VII) sorption and reduction.

The applicability of the Langmuir adsorption model for the Au(III) and Re(VIII) sorption-reduction does not revoke the real multi-step character of the processes. In this connection, the K_L parameter is the empirical coefficient rather than the equilibrium constant of the definitely specified reaction. The Langmuir adsorption model implies the simple stoichiometry of interactions. Although, as far as the real overall reaction is more complicated, the determination of the equilibrium constant through fitting the experimental data by the Langmuir equation becomes invalid. After that, the trustworthiness of the ΔH and ΔS estimates raises doubts.

Reduction Phenomenon

Because of the issues raised above, the reduction phenomenon has to be analyzed from different angle. In accordance to Bard,[49] reduction potential of Au(III) and Re(VII) in acidic solutions is determined as +1.002 and +0.415 eV, respectively. That fact implicates the conclusion that if, in present studies, "less negative potential" gold has been reduced to its metallic form, there is high possibility of Re(VII) ion reduction as a "more negative potential" metal. The same conclusion has been made by Park[53] who proceeded different process of Au(III) and Pd(II) reduction-coupled removal from hydrochloride solutions using crosslinked chitosan beads.

In order to confirm the assumption that reduction of Au(III) acted on the Dowex M4195 resin's surface, images of the samples loaded with gold chlorocomplex ($AuCl_4^-$) and rhenium ion (ReO_4^-) were captured. The investigation was proceeded using Joel JSM5800LV scanning electron microscope equipped with an energy-dispersive spectrometer (EDS).

Figure 7 displays SEM photographs of the Dowex M4195 resin loaded with Au(III) (a, a′) and Re(VII) (b, b′). In the panels, a and a′ (Figure 7) gold microplates can be observed on the surface of the polymer bead; furthermore, panel a′ shows presence of the metallic gold in the fracture of the bead of the resin. Although there are no visible signs of the presence of the metallic rhenium on the surface and fractures [Figure 7(b,b′)]. Nevertheless, the morphology of the surface of the Dowex M4195 resin loaded with gold [Figure 7(a′)] seems to be porous, while there are no pores visible on a smooth surface of the resin after sorption of rhenium process. As previously mentioned, basing on the sorption isotherms (Figures 1–3) absence of the plateau of the sorption of Au(III) isotherm was probably caused by the constant reduction of gold to its metallic form that proceeded even after separation from the resin bed. The SEM image [Figure 7(b′)] indicates, that rhenium ion Re(VII), loaded on the Dowex M4195 could transform to the oxide form that prevent access to the functional groups of the resin by filling up the pores. That could be the reason why the sorption isotherms (Figures 1–3) display plateau curve of the rhenium sorption. Reduction of Re(VII) ion to its lower oxidation state, if occurred, could be limited by accessibility to the surface of the resin.

Table II. Energy of Activation

Metal	E_a (kJ·mol^{-1})
Au	−29.92
Pt	22.47
Pd	36.23
Re	−38.83

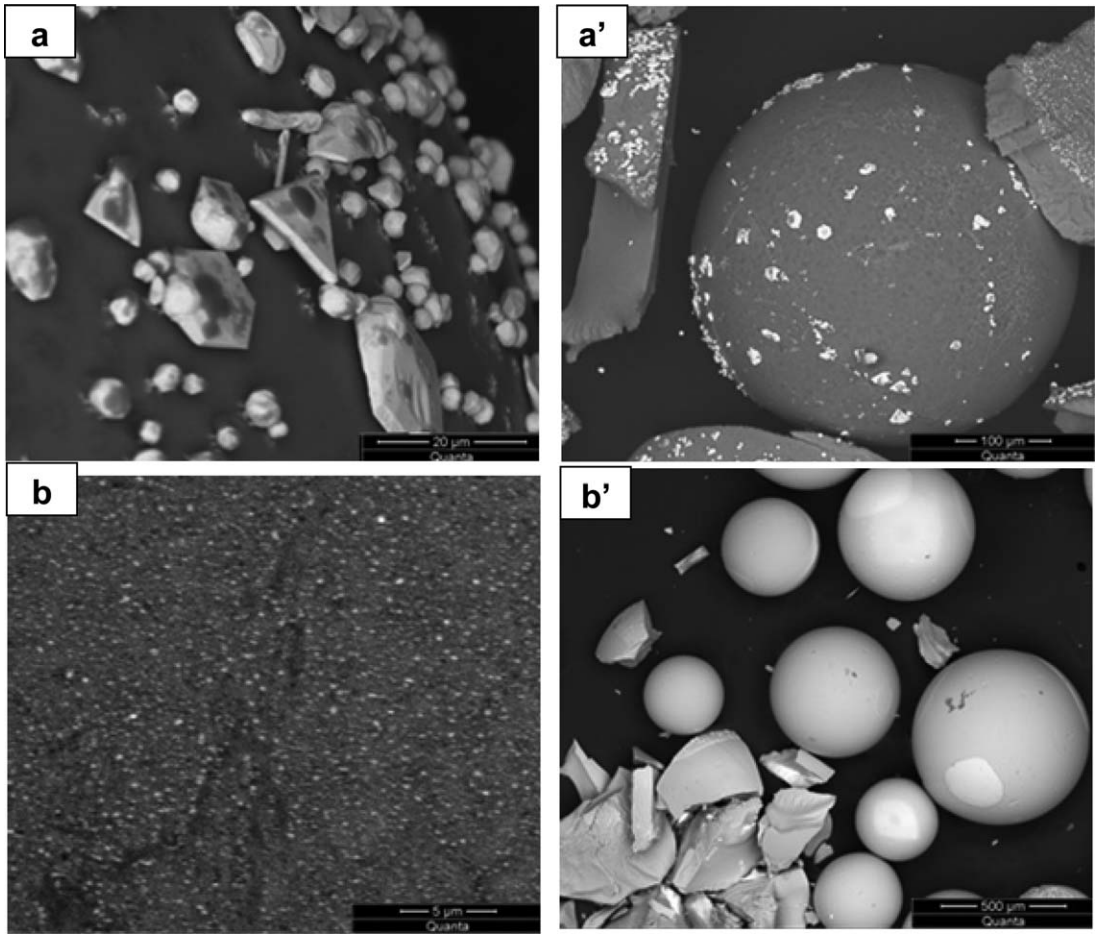

Figure 7. SEM images of the Dowex M4195 resin loaded with gold (a, a′) and rhenium (b, b′).

Figure 8 displays the SEM/BSE picture of the single gold microplate. Because of the clear material contrast it is possible to measure its size that is placed between 13 µm in its narrowest and 15 µm in its widest part. The determination of the thickness of the microplate is difficult and requires a nano-tweezers that are extremely rare. Therefore, we were unable to measure that dimension. Although, we have attempted to capture TEM images of the sample, unfortunately, the microstructures were thick enough to be not transparent.

The attached to the equipment EDS allowed retrieving data about elemental composition of the Dowex M4195 surface, expressed with the atomic percentage. Figure 9 gives EDAX surface analysis of the unsaturated resin (a) and loaded with gold (b) and rhenium (c) as well. The data confirms the presence of the Au and Re on the surface of the resin regardless to their species distribution. After sorption of Au(III) significant increase of the chlorine content is observed [Figure 9(b)]. Greater amount of the chlorine in sample loaded with gold (a) could be caused by presence of the metal in the chlorocomplex form ($AuCl_4^-$) while increasing content of oxygen in case of the sample saturated with rhenium [Figure 9(c)] may be attributed to the fact that Re exists in the form of its oxo species. Increasing contribution of the oxygen observed on the surface composition of the resin loaded with gold [Figure 9(b)] suggests that reduction of the gold was followed by oxidation of the surface of the resin. Furthermore, because of the rocketing value of oxygen [Figure 9(c)], its presence in the sample loaded with

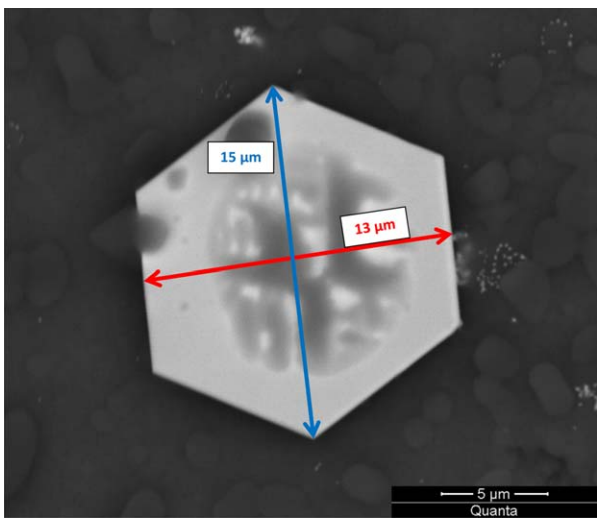

Figure 8. SEM/BSE image of a gold microplate localized on the Dowex M4195 resin's surface. [Color figure can be viewed in the online issue, which is available at wileyonlinelibrary.com.]

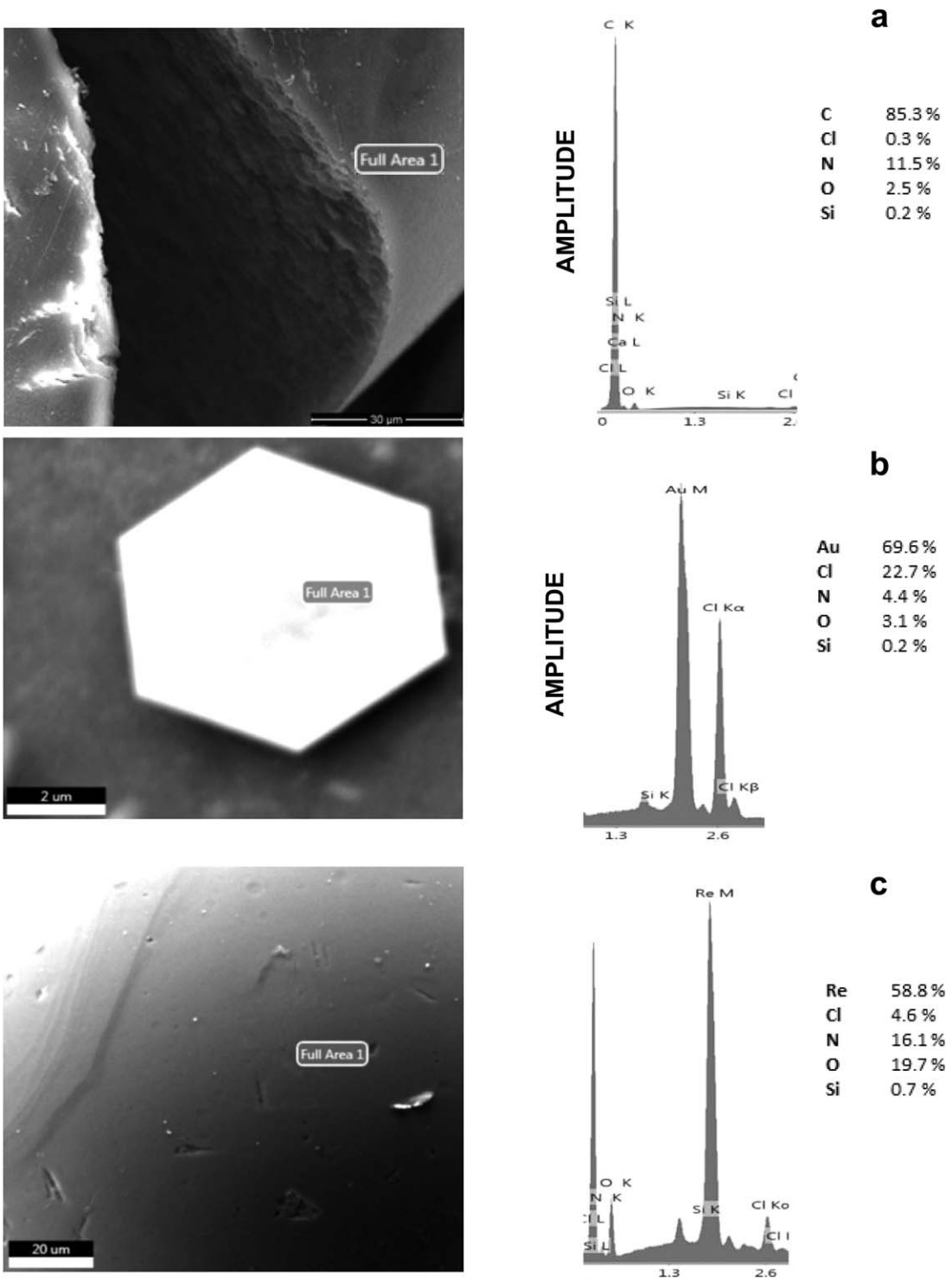

Figure 9. EDAX analysis of the unsaturated Dowex M4195 resin (a), loaded with gold (b) and rhenium (c).

rhenium may be attributed not only to the ReO_4^- ion and its other species. There is possibility that oxidation of the resin surface could occur during rhenium sorption as well. Furthermore, there are some hard to define structures present on the zoomed surface of the Dowex M4195 loaded with rhenium [Figure 7(b)]. In that circumstances reduction of Re(VII) could be possible.

In order to prove or exclude presence of the metallic gold and rhenium within the structure of the Dowex M4195 resin, the XRD studies were performed. It has been done by registering X-ray diffraction patterns (Cu $K^{\alpha} = 1.5418$ A). The XRD patterns of virgin and saturated Dowex M4195 resin recorded in the 2θ range from 3 to 100° are shown in the Figure 10. The comparison of the experimental data with metallic gold standard pattern

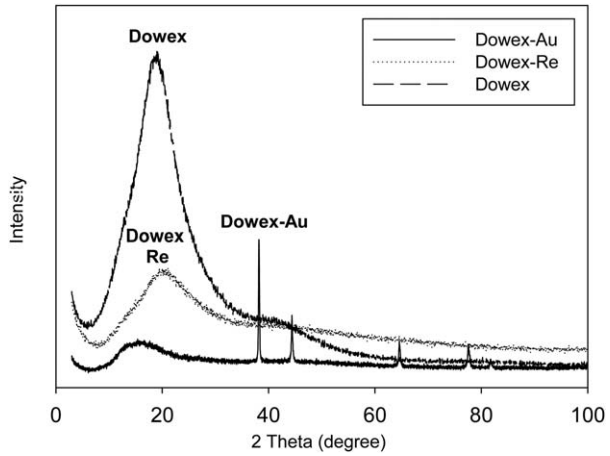

Figure 10. The XRD patterns of the Dowex M4195 resin

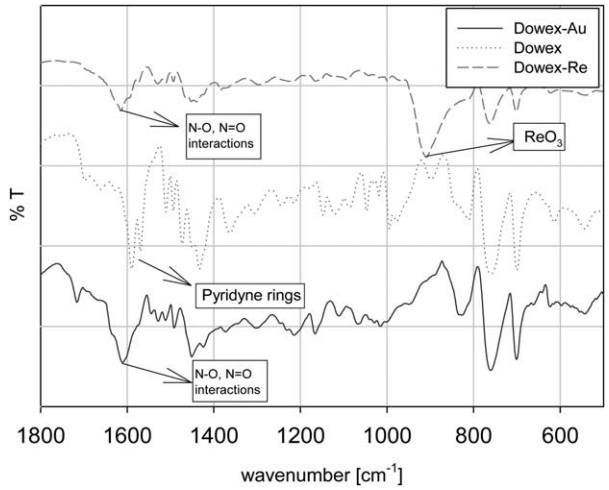

Figure 11. The FTIR spectra of the Dowex M4195 resin.

(card number: 04–0784) from ICDD database can be seen in the Supporting Information Figure S5. The graph show, that the obtained during present studies microstructures reveal the same crystalline structure as the standard gold.

Characteristic peaks (Dowex M4195 Au, Figure 10) appearing at 2θ =38.18°, 44.38°, 64.58°, 77.55°, and 81.71° are proving formation of gold microstructures in the proceeded sample. Peak positions indicate the presence of crystalline metallic gold. The peaks correspond to the {111}, {200}, {220}, {311}, and {222} lattice fringes of a facecentered cubic (fcc) structure. The unit cell parameters for the standard are: $a = 0.4079$ nm, cell angle = 90°, $Z = 4$, and the space group is Fm3m.

Although, there was no metallic rhenium detected in the investigated, loaded with that metal resin (Dowex M4195 Re). Although, previous considerations suggest that reduction of that metal could occur, therefore further analyses were executed.

In order to verify if oxidation state of rhenium have changed during sorption process, we have proceeded desorption of that metal using the previously saturated Dowex M4195 resin, and the best techniques based on our experience.[27] Determined desorption reached only 50% which means, that most of the uptaken rhenium existed in different than ReO_4^- form (changed its oxidation state), and, as the result could not be desorbed.

The FTIR analysis allowed determining changes in the structure of the Dowex M4195 resin after sorption of Au(III) and Re(VII) processes. Figure 11 gives recorded spectra in restricted range of 500–1800 cm^{-1}. Strong bands at 1589 and 1569 cm^{-1} (Dowex M4195, Figure 11) correspond to the interactions in the pyridine rings located in the bis (2-pyridylmethyl)amine functional groups of the resin.[54] After sorption processes that area has been transformed, and new bands at 1610 cm^{-1} (Dowex M4195 Au, Figure 11) and 1614 cm^{-1} (Dowex M4195 Re, Figure 11) appear. Those peaks correspond to the interactions between nitrogen and oxygen atoms (N-O, N=O).[55,56] That fact suggests that functional groups of the Dowex M4195 resin could be oxidized during uptake of gold and rhenium processes. In order to verify that suspicion, the unsaturated bis (2-pyridylmethyl)-amine functional groups of the Dowex M4195 resin have been transformed to the pyridine N-oxide derivatives with use of the method described in Ref. [57. Then, the FTIR spectra of the oxidized resin have been executed. Recorded spectra (Figure 12) display the same phenomenon as that, observed after sorption of gold and rhenium. After oxidation process, strong bands at 1589 and 1569 cm^{-1} (Dowex M4195, Figure 11) have been replaced by the new one at 1604 cm^{-1} (Dowex M4195-Ox, Figure 12). Taking into account that fact, there is a possibility that during sorption of Au(III) and Re(VII) functional groups of the resin has been oxidized to the pyridine N-oxide derivatives.

The phenomenon was followed by reduction of gold which was present in its metallic form in the structure of the resin [Figure 7(a)]. On the other hand, rhenium behavior is not so obvious, there is a possibility that reduction of Re(VII) could lead to different, nonmetallic species. Appearance of the very strong band at 909 cm^{-1} (Dowex M4195 Re, Figure 11) has been previously reported[58] as indicator of the ReO_3 presence. That could mean that rhenium has been reduced to the +6 oxidation state and took the form of its oxide.

To further examine the phenomenon, the Raman's studies have been performed. Figure 13 displays recorded spectra of the unloaded and loaded with rhenium Dowex M4195 resin and

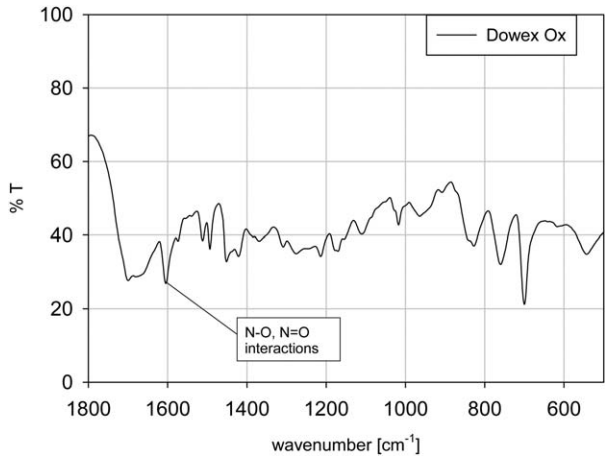

Figure 12. The FTIR spectra of the oxidized Dowex M4195 resin.

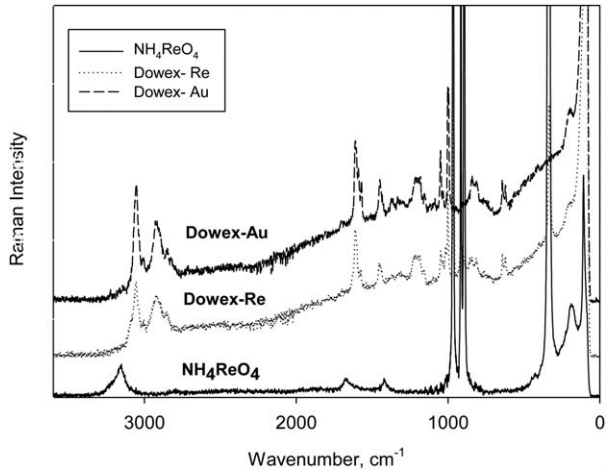

Figure 13. The Raman's spectra of the rhenium-saturated Dowex M4195 resin.

standard NH_4ReO_4 as well. Strong bands at 1610, 1590, and 1570 cm^{-1} (Dowex, Figure 13) reveal, as the FTIR spectra (Figure 11), presence of the pyridine rings derived from the bis (2-pyridylmethyl)amine functional groups of the resin.[59] After sorption of rhenium process, intensity of those peaks significantly decreases and a new band, responsible for the N-O bonds (assigned to pyridine N-oxide derivatives), at 856 cm^{-1} appears (Dowex-Re, Figure 13).[59] The corresponding phenomenon has been observed in the recorded FTIR spectra (Figure 11). That could mean that functional groups of the Dowex M4195 resin has been partially oxidized during rhenium uptake process, and, if so, some element had to be reduced. According to Biswas[60] and Pikl[61] strong bands at 962, 912, and 333 cm^{-1} that appeared after sorption of rhenium (Dowex-Re, Figure 13) correspond to the stretching vibrations between rhenium and oxygen in the ReO_3. The same observation has been made by Castriota *et al.*,[62] who registered similar peaks in ReO_3 Raman's spectra. Although they[62] indicate that such bands can be also generated by grouped in organized structures ReO_4^- ions. Basing on the attached to the Figure 13 NH_4ReO_4 spectrum, that conclusion is applicable to the present studies. Bands assigned to the ReO_3 (Figure 13, Dowex-Re) appears with different intensity also on the standard spectrum (Figure 13, NH_4ReO_4). Therefore, the executed spectra are not enough for determination of the nature of the reduction of rhenium.

In order to definitely prove or exclude reduction of Au(III) and Re(VII) it was necessary to determine elements and their oxidation states on the loaded with gold and rhenium surface of the Dowex M4195 resin. For that reason the XPS analyses were employed. Figure 13 displays recorded XPS spectra of the Dowex M4195 resin loaded with gold (b) and rhenium (c). Furthermore, a survey scan of the both samples has been performed [Figure 14(a)].

In the spectra, Au 4f [Figure 14(b)] doublet peaks $4f_{7/2}$, $4f_{5/2}$ (87.25 and 90.92 eV), responsible for Au(III), are dominating. These energies have been previously assigned to the $HAuCl_4$ used for the proceeded sorption process.[63] Its amount, basing on the proceeded XPS analysis has been estimated as 75.4% of

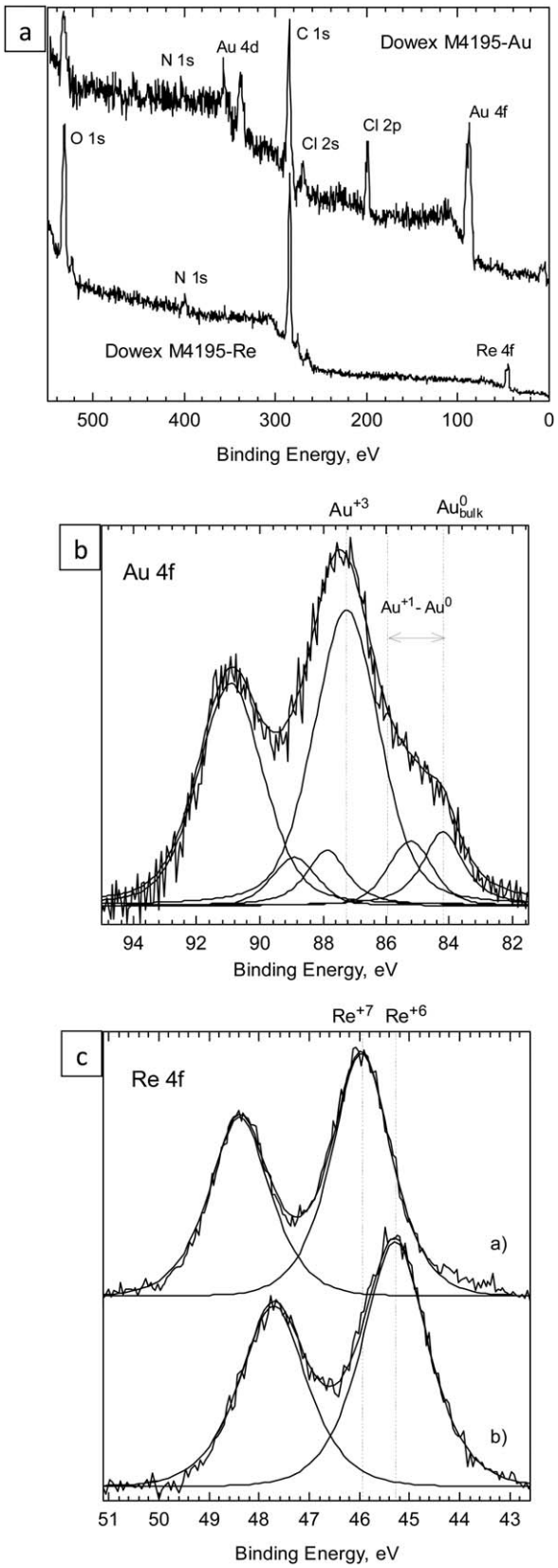

Figure 14. XPS spectra of the Dowex M4195 resin saturated with gold and rhenium; (a) survey scan, (b) resin loaded with gold, (c) resin loaded with rhenium.

the total amount of gold adsorbed on the surface of the Dowex M4195 resin. In the area of lower energies [Figure 14(b)] peaks at 84.2 and 87.87 eV, characteristics of the $Au(0)_{bulk}$ have been distinguished.

These components do not cover in a satisfactory manner the whole Au4f spectrum. It was necessary to take into account one more area in the range of approximately 84–86 and 88–90 eV that identification is not entirely clear: within that range, bonds of both, Au(I) and A(0) are being detected: the effect is attributed to the fact, that the smaller particles of $Au(0)_{surface}$ are, the greater energy of their bonds is.[64] To these forms, Au(I) and $Au(0)_{surface}$, the binding energies 85.24 and 88.91 eV, respectively, have been conventionally assigned. Ultimately, their content is estimated as 11.4% of Au(I) and 13.3% of $Au(0)_{bulk}$.

The results of the XPS analyses have been confronted with the XRD, EDS, SEM, and digital–optical microscopy. It turned out, that XRD tests did not reveal a presence of the Au(III) and Au(I). Instead, great clusters of microplates and small amount of green powder (assigned to the presence of the AuCl) are visible. That means that Au(III), adsorbed on the surface of the resin, has been uptaken directly from a solution creating a dispersed amorphous phase. Moreover, partial reduction to the Au(I) does not lead to greater dimensions of the Au particles as well as arrangement of the gold structures. As the result the Au(III) and Au(I) had not been detected during the XRD analysis, instead, they have been recorded by XPS technique.

The crystallographic structure of the metallic gold causes, that it is possible to detect it using the XRD method irrespectively of their size. Although, progressive reduction of Au(III) to metallic gold leads to an agglomeration of Au(0) particles significantly understating the amount of metallic gold detected by XPS. For instance, for applied simplified model of flat, homogenous Au(0) microplates that thickness is set as 50 nm, the undervaluation may be tenfold, while for microplates 100 nm thick the undervaluation is estimated as 20fold. These values have been estimated taking the inelastic mean free path way (IMFP) of fotoelectrons Au 4f in Au, that kinetic energy is 1170 eV and $\lambda = 1.55$ nm, which means the maximum depth of sampling $3\lambda \approx 5$ nm.[65]

Binding energies Re $4f_{7/2}$ and Re $4f_{5/2}$ in the investigated sample [Figure 14(c)] have been decreased, comparing to a reference NH_4ReO_4 (powder), by 0.7 eV and are being determined as 45.29 and 47.72 eV. That change is interpreted as reduction of rhenium Re(VII) to Re(VI), that form, confronting with the previous analyses, is probably ReO_3.

Rhenium creates diversified oxide forms: ReO_2, ReO_3, and Re_2O_7 that binding energies rise with increasing oxidation state of Re. According to the available database NIST, average binding energies of these species, for electrons Re $4f_{7/2}$ are: 43.03, 45.37, and 46.65 eV, respectively.[66]

In the authors' own research binding energies Re $4f_{7/2}$ for Re immobilized on the Al_2O_3 support were 43.0, 45.0, and 46.5 eV, respectively. Although, that last value for bulk Re_2O_7 was slightly greater and amounted as 47.1 eV.[67] Progressive reduction of Re(VII) in a form of Re_2O_7 to ReO_3 and further to ReO_2 was observed by another authors as well.[68] They assigned to the ReO_3 and ReO_2 energies of Re $4f_{7/2}$ bonds, that values were 45.5 and 42.5 eV, respectively.

Referenced literature data and own XPS analyses lend credence to the conclusion that Re(VII) has been reduced to the Re(VI). Furthermore, detail analysis of the Re 4f spectra [Figure 14(c)], that is FWHM and required ratios of the $4f_{5/2}$ and $4g_{7/2}$ peaks ($4f_{5/2}$:$4f_{7/2} = 0.75$) suggests the homogenous form of Re, present on the surface of the Dowex M4195 resin, which means that Re(VII) reduced to the Re(VI) entirely. Moreover, no Re(IV) has been observed.

CONCLUSIONS

The ability of the Dowex M4195 resin for reduction-coupled noble metals sorption was evaluated. As side effect gold microplates formation was observed.

Determined mechanism of the ReO_4^- removal process, reduction potential value of Re(VII) ions, and executed analyses suggest that reduction of rhenium to the +6 oxidation state probably occurred during present studies.

Reduction of the Au(III) and Re(VII) was probably followed by the oxidation of the Dowex M4195 resin's functional groups to the pyridine N-oxide derivatives.

ACKNOWLEDGMENTS

This work was financed by a statutory activity subsidy from the Polish Ministry of Science and Higher Education for the Faculty of Chemistry of Wroclaw University of Technology.

REFERENCES

1. Hageluken, C. *Acta Metallurgica Slovaca* **2006**, *12*, 111.
2. Burke, M. *Chem. World* **2007**, *4*, 45.
3. Official Journal of European Union **2012**, *197*.
4. Park, Y. J.; Fray, D. J. *J. Hazard. Mater.* **2009**, *164*, 1152.
5. Lito, P. F.; Cardoso, S. P.; Loureiro, J. M.; Silva, C. M. Ion Exchange Technology I; Springer: London, **2012**.
6. Liang, P.; Yuana, L.; Yangb, X.; Zhouc, S.; Huang, X. *Water Res.* **2013**, *47*, 2523.
7. Nasefa, M. M.; Güven, O. *Prog. Polym. Sci.* **2012**, *37*, 1597.
8. Harris, N. D. U.S. Patent 3872067 **1975**.
9. Parajuli, D.; Khunathai, K.; Adhikari, R. C.; Inoue, K.; Ohto, K.; Kawakita, H.; Funaoka, M.; Hirota, K. *Miner. Eng.* **2009**, *22*, 1173.
10. McGillicuddy, N.; Nesterenko, E. P.; Nesterenko, P. N.; Jones, P.; Paull, B. *J. Chromatogr. A* **2013**, *1276*, 102.
11. Dasbasi, T.; Sacmaci, S.; Sahan, S.; Kartal, S.; Ulgen, A. *Talanta* **2013**, *103*, 1.
12. Sacmaci, S.; Kartala, S.; Yılmaza, Y.; Sacmaci, M.; Soykan, C. *Chem. Eng. J.* **2012**, *181-182*, 746.
13. Marinho, S. R.; Silva, C. N. d.; Afonso, C. J.; Cunha, S. W. D. *J. Hazard. Mater.* **2011**, *192*, 1155.
14. Tuzen, M.; Saygi, K. O.; Soylak, M. *J. Hazard. Mater.* **2008**, *156*, 591.

15. Dozol, H.; Méŕiguet, G.; Ancian, B.; Cabuil, V.; Xu, H.; Wang, D.; Abou-Hassan, A. *J. Phys. Chem. A* **2013**, 20958.
16. Tai-Lin, L.; Hsing-Lung, L. *Int. J. Mol. Sci.* **2013**, *14*, 9834.
17. Sakai, T.; Horiuchi, Y.; Alexandridis, P.; Okadaa, T.; Mishima, S. *J. Colloid Interface Sci.* **2013**, *394*, 124.
18. Changmei, S.; Guanghua, Z.; Chunhua, W.; Rongjun, Q.; Ying, Z.; Quanyun, G. *Chem. Eng. J.* **2011**, *172*, 713.
19. Wang, L.; Chen, X.; Zhan, J.; Chai, Y.; Yang, C.; Xu, L.; Zhuang, W.; Jing, B. *J. Phys. Chem. B* **2005**, *109*, 3189.
20. Kan, C.; Zhu, X.; Wang, G. *J. Phys. Chem. A* **2006**, *110*, 4651.
21. Au, L.; Lim, B.; Colletti, P.; Jun, Y.; Xia, J. *Chem. Asian J.* **2011**, *5*, 123.
22. Lin, G.; Lu, W.; Cui, W.; Jiang, L. *Cryst. Growth Des.* **2010**, *10*, 1118.
23. Burguete, M. I.; García-Verdugo, E.; Luis, S. V.; Restrepo, J. A. *Phys. Chem. Chem. Phys.* **2011**, *13*, 14831.
24. Cyganowski, P.; Jermakowicz-Bartkowiak, D. *Sep. Sci. Technol.* **2014**, *49*, 1689.
25. Wolska, J.; Bryjak, M. *Desalination* **2011**, *283*, 193.
26. Leonard, J.; Lygo, B.; Procter, G. Advanced Practical Organic Chemistry, 3rd ed.; CRC Press: New York, **2013**.
27. Jermakowicz-Bartkowiak, D.; Kolarz, B. N. *React. Funct. Polym.* **2011**, *71*, 95.
28. Mendham, J.; Denney, R. C.; Barnes, J. D.; Thomas, M. J. K. Vogel's Quantitative Chemical Analysis (6th ed.); Pearson Education Limited: Beijing, **2000**.
29. Cyganowski, P.; Jermakowicz-Bartkowiak, D. *Sep. Sci. Technol.* **2014**, *49*, 1689.
30. Jermakowicz-Bartkowiak, D.; Kolarz, B. N.; Serwin, A. *React. Funct. Polym.* **2005**, *65*, 135.
31. Foo, K. Y.; Hameed, B. H. *Chem. Eng. J.* **2010**, *156*, 2.
32. Atkins, P.; Paula, J. Atkins' Physical Chemistry; Oxford University Press: Oxford, **2010**.
33. Shen, X. E.; Shan, X. Q.; Dong, D. M.; Hua, X. Y.; Owens, G. *J. Colloid Interface Sci.* **2009**, *330*, 1.
34. Ho, Y. S. *Scientrometrics* **2004**, *59*, 171.
35. Schiewer, S.; Patil, S. B. *Bioresour. Technol.* **2008**, *99*, 1896.
36. Ho, Y. S. *J. Hazard. Mater.* **2006**, *136*, 681.
37. Shi, K.; Wang, X.; Guo, Z.; Wang, S.; Wu, W. *Colloids Surf. A* **2009**, *349*, 90.
38. Lesniewicz, A.; Gackiewcz, L.; Zyrnicki, W. *Int. Biodeterior. Biodegrad.* **2010**, *64*, 81.
39. Diniz, C. V.; Doyle, F. M.; Ciminelli, V. S. T. *Sep. Sci. Technol.* **2006**, *37*, 3169.
40. Bernardis, F. L.; Grant, R. A.; Sherrington, D. C. *React. Funct. Polym.* **2005**, *65*, 205.
41. Wolowicz, A.; Hubicki, Z. *Chem. Eng. J.* **2010**, *160*, 660.
42. Zagorodnyaya, A. N.; Abisheva, Z. S.; Sharipova, A. S.; Sadykanova, S. E.; Bochevskaya, Y. G.; Atanova, O. V. *Hydrometallurgy* **2013**, *131-132*, 127.
43. Mohammadnejad, S.; Provis, J. L.; Deventer, J. S. J. *J. Colloid Interface Sci.* **2013**, *389*, 252.
44. Grace, A. N.; Pandian, K. *Colloids Surf. A* **2007**, *302*, 113.
45. Sakai, T.; Ishigaki, M.; Okada, T.; Mishima, S. *J. Nanosci. Nanotechnol.* **2010**, *10*, 916.
46. Zhang, F.; Liu, N.; Zhao, P.; Sun, J.; Wang, P.; Ding, W.; Liu, J.; Jin, J.; Ma, J. *Appl. Surf. Sci.* **2012**, *263*, 471.
47. Bolisetty, S.; Vallooran, J. J.; Adamcik, J.; Handschin, S.; Gramm, F.; Mezzeng, R. *J. Colloid Interface Sci.* **2011**, *361*, 90.
48. Nguyen, D. T.; Kim, D. J.; So, M. G.; Kim, K. S. *Adv. Powder Technol.* **2010**, *21*, 111.
49. Bard, A. J.; Parsons, R.; Jordan, J. Standard Potentials in Aqueous Solutions; IUPAC (Marcel Dekker): USA, New York, **1985**.
50. Mozurkewich, M.; Benson, S. W. *J. Phys. Chem. A* **1984**, *88*, 6429.
51. Karaoglu, M. H.; Zor, S.; Ugurlu, M. *Chem. Eng. J.* **2010**, *159*, 98.
52. Saha, P.; Chowdhury, S. Insight into Adsorption Thermodynamics; InTech: Durgapur, India, **2011**.
53. Park, S.; Kwak, I.; Won, S. W.; Yun, Y. *J. Hazard. Mater.* **2013**, *248-249*, 211.
54. Li, L.; Goh, S. H. *J. Polym. Sci. Part B: Polym. Phys.* **2002**, *40*, 1125.
55. Stuart, B. Infrared Spectroscopy-Fundamentals and Applications; Wiley: Chichester, **2004**.
56. McCarthy, S. A.; Davies, G. L.; Gun, Y. K. *Nature (London)* **2012**, *7*, 1677.
57. Soykan, C.; Coskun, R.; Delibas, A. *Thermochim. Acta* **2007**, *456*, 152.
58. Nikonova, O. A.; Nedelec, J. M.; Kessler, V. G.; Seisenbaeva, G. A. *Langmuir* **2011**, *27*, 11622.
59. Colthup, N. B.; Daly, L. H.; Wiberley, S. E. Introduction to Infrared and Raman Spectroscopy; Academic Press: New York, **1990**.
60. Biswas, K.; Bhat, S. V.; Rao, C. N. R. *J. Phys. Chem. C* **2011**, *111*, 5689.
61. Pikl, R.; Weber, K.; Sundermeyer, J.; Herrmann, W. A.; Kiefer, W. *Vib. Spectrosc.* **1997**, *14*, 299.
62. Castriota, M.; Cazzanelli, E.; Das, G.; Kalendarev, R.; Kuzmin, A.; Marino, S.; Mariotto, G.; Purans, J.; Scaramuzza, N. *Mol. Cryst. Liq. Cryst. Sci. Technol. Sect. A* **2007**, *474*, 1.
63. Kwak, I. S.; Bae, M. A.; Won, S. W.; Mao, J.; Sneha, K.; Park, J.; Sathishkumar, M.; Yun, Y. S. *Chem. Eng. J.* **2010**, *165*, 440.
64. Cuenya, B. R. *Thin Solid Films* **2010**, *518*, 3127.
65. Powell, C. J.; Jablonski, A. NIST Electron Inelastic-Mean-Free-PathDatabase ver. 1.2, SRD 71 National Institute of Standard and Technology: Gaithersburg, **2010**.
66. NIST Standard Reference Database 20, Version 4.1; Available at: http://srdata.nist.gov/xps, access date April, 1st **2015**.
67. Okal, J.; Tylus, W.; Kepinski, L. *J. Catal.* **2004**, *2005*, 498.
68. Yuan, Y.; Shido, T.; Iwasawa, Y. *Chem. Commun. (Cambridge)* **2000**, *15*, 1421.